



# The Detection of Glaucoma in Fundus Images Based on Convolutional Neural Network

Ali Yakoob Al-Sultan<sup>1,\*</sup>

<sup>1</sup>Department of Computer, College of Science for Women, University of Babylon, Babylon, Iraq

Emails: [ali.alsultan@uobabylon.edu.iq](mailto:ali.alsultan@uobabylon.edu.iq)

## Abstract

Glaucoma is a common disease affecting the human retina, primarily caused by elevated intraocular pressure. Early intervention is crucial to prevent damage to the affected organs, which could lead to their dysfunction. This paper focuses on enhance diagnosis accuracy of the system to determine if a patient is at risk of developing glaucoma. In this paper a novel convolutional neural network (CNN) designed, specifically for the detection of glaucoma in fundus images. This architecture optimizes for the unique characteristics of fundus imagery, enhancing detection accuracy, and also compiled a large and diverse dataset of fundus images, crucial for training and validating our CNN model. The dataset includes a significant number of images with detailed annotations, ensuring robust model training. In addition, implemented sophisticated image preprocessing methods to enhance the quality of the fundus images. These techniques, including noise reduction and contrast enhancement, significantly improve the input data quality for the CNN. The system operates in three stages. First, it preprocesses the image by cropping, enhancing, and resizing it to a consistent 256×256 pixels. Next, it employs an advanced feature extraction to analyses key features of the optic disc and optic cup in retinal images. Finally, the Soft-Max function classifies the images, identifying those with glaucoma and distinguishing them from normal eye samples. The model's performance was thoroughly evaluated using various metrics like accuracy, Sensitivity, specificity, and the area under the curve are metrics used to evaluate the performance of a diagnostic test. Sensitivity measures the test's ability to correctly identify positive cases, specificity assesses its accuracy in identifying negative cases, and the area under the curve indicates the overall effectiveness of the test across different thresholds. The results achieved by the proposed system were thoroughly analyzed, revealing a high accuracy rate in glaucoma classification, reaching 99%.

**Keywords:** Glaucoma; Convolution neural network CNN; Medical imaging; Deep learning, Ocular Disease Intelligent Recognition

## 1. Introduction

Glaucoma is the most severe and prevalent illness affecting the human eye. Glaucoma is a long-term condition that causes damage to the optic nerve, and it is the second leading cause of blindness and visual loss. [1][2]. This illness can potentially cause irreversible blindness [3]. By 2020, 80 million individuals will have glaucoma [4], increasing to 111.8 million in 2040, aging from 40-80 years [5]. There are superfluities associated with glaucoma, including very high intraocular concentrations inside the human eye, which are known to be harmful to both the blood vessels and the optic nerve. Eye physicians who do eye illness tests must be highly competent and have enough time to identify the condition [6]. Given the growing number of individuals suffering from glaucoma, depending on medical equipment to identify and detect the illness may become impractical [7]. Extensive research is being conducted utilizing different image processing methods to address the early identification of glaucoma issues [8]. Table (1) depicts a normal fundus image vs. glaucoma from several datasets. In recent research, the National Eye Institute (NEI) discovered that the estimated rise in glaucoma patients is concerning compared to

previous years. With a significant increase in individuals suffering from glaucoma and DR, early identification of these eye illnesses is critical for early detection of glaucoma and DR. Therefore, earlier treatment may avoid irreversible blindness. Nonetheless, many patients are unaware of the disease until it has progressed to a dangerous level [9].

## 2. Related Work

Ajitha S., M V Judy, et al. [10] In this study, an automated glaucoma screening framework using an Alexnet model and SVM classifier to enhance the accuracy of classification. In this study, three datasets were used (Drishti\_GS1, Origa, and HRF). The obtained accuracy is 91.21%. Baidaa Al-Bander et al. [11] present an automated approach based on a convolutional neural network that can distinguish the eye with glaucoma from the unaffected. The feature is extracted from images using CNN, and then the SVM is used for classification. The results were 88.2% accuracy, 90.8 % specificity, and 85% sensitivity, respectively.

Ravi Kumar Gupta, Utkarsh Sharma, et al. [12] The proposed model for Deep Learning consists of six layers: four convolution layers and two fully functional levels. To improve the precision of glaucoma diagnosis, discontinuation and augmentation techniques are utilized. Details on ORIGA and SCES have been rigorously examined. Mary, J. et al. [13] Construct a CNN-based system for the automated diagnosis of glaucoma using deep learning. The proposed architecture has six learning techniques, including four convolutional strata and two fully interconnected strata. The results demonstrate that the recipient's area under the curve, (called shortly AUC) is much greater than the recent methods in the detection of glaucoma disease with 0.831 for the ORIGA and 0.887 for the SCES databases respectively. Silvia Ovreiu, et al. [14] in this work the residual networks were used to identify the early stages of glaucoma and to launch an exclusive dataset of early-stage glaucoma fundus images. The ResNet50 network, which at first received its training on the ImageNet dataset.

On the validation set, the degree of accuracy reached a level of 96.95%. Orlando, José Ignacio, et al. [15] Provide results from a feasibility study using pre-trained CNNs built from data sources other than medical records for automatic glaucoma diagnosis. The fundus images were fed into two CNN, Over-Feat and VGG-S, which then generated feature vectors. The area under the average ROC curve was utilized to evaluate the results on the Drishti-GS1 dataset. Serte, Sertan, et al. [16] this article describes an algorithm of deep learning for diagnosing glaucoma using fundus images. Unlike earlier research, this model was applied to various datasets and architectures. The findings indicate that the model is 80% superior to the previous work in the literature.

## 3. Material and Methods

### 3.1 Main Dataset Description

A structured ophthalmic database, Ocular Disease Intelligent Recognition (ODIR) has information on over 5,000 cases, including their ages of fundus images. This data collection is collected by the company from several Chinese medical facilities. The dataset divides people into eight categories according to their health: normal (N), diabetic (D), glaucoma (G), cataract (C), AMD (A), hypertensive (H), myopic (M), and other (O). The proposed system deal with glaucoma disease only; therefore, 1030 fundus image were taken from the ODIR dataset and split into 70% training and 30% testing; Table (1) shows the images separated into their various ODIR datasets These datasets are useful for a wide variety of different types of study. [17][18][19].

**Table (1)** Statistics of ODIR dataset

	<b>Glaucoma</b>	<b>Normal</b>	<b>Total</b>
<b>Train</b>	210	500	710
<b>Test</b>	155	165	320
<b>Total</b>	365	665	1030

### 3.2 Other Datasets

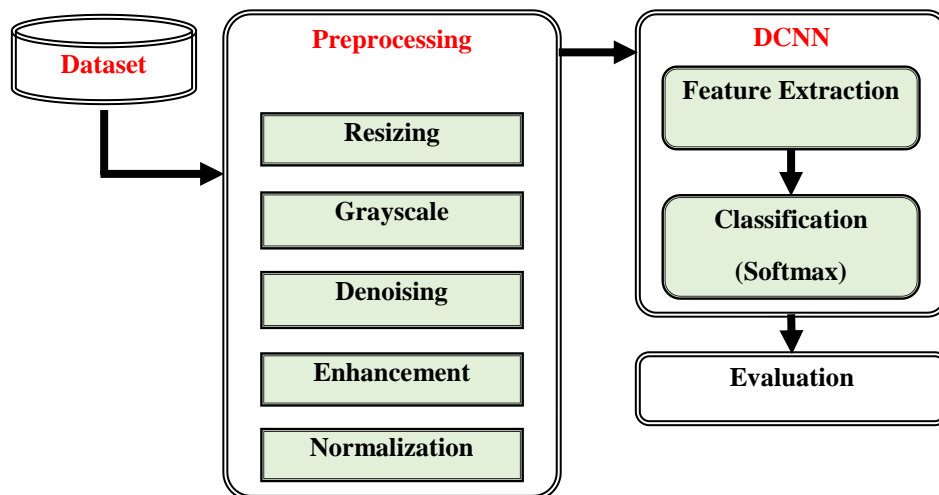
The proposed system was evaluated using multiple standard datasets and its performance was compared with previous studies. Five additional public databases were utilized in this work: the sjchoi86-HRF database containing 401 images, the HRF database with 45 images, and the ACRIMA database with 705 images; RIM-ONE [23], with 455 images; ORIGA [24], and Drishti-GS1 [25], with 101 samples. Table (2) show the details of these datasets.

**Table (2)** Datasets details of glaucoma disease

Database	Glaucoma	Normal	Total
ODIR [19]	365	665	1030
Sjchoi86-HRF [20]	101	300	401
HRF [21]	27	18	45
ACRIMA [22]	396	309	705
RIM-ONE [23]	194	261	455
ORIGA [24]	168	482	650
Drishti-GS1 [25]	70	31	101

#### 4. Methodology

The suggested method may be subdivided into three stages. This is the first stage is the images dataset preprocessing stage, which contains several prepared images before being handled by the CNN model. These stages start by resizing all dataset images into (256\*256) pixels, converting color images to greyscale images, and minimizing the effect of noise with a mean filter. The contrast-limited adaptive histogram equalization “CLAHE” [26] will be used to improve the contrast. To achieve this effect, scale the image size by 255. In the second step, crucial features are extracted from the collected fundus images by CNN. In the last step, these features are used to label the fundus images as either normal or glaucoma. Figure 1 show the block diagram of the proposed system. The details of preprocessing as the following:

**Figure 1.** The block diagram of the proposed system

**A. Pre-processing:** An integral part of the glaucoma detection system is the pre-processing phase. All of the dataset's fundus images have undergone this procedure to prepare them for the training phase and to set the stage for feature extraction. All images are converted to greyscale images, resized to (256\*256) pixels, denoised by a mean filter, enhanced with CLAHE, and normalized by dividing by 255.

#### **Algorithm (1): Pre-processing operations**

Input: CT scan images.

Output: Resized image # (256 \* 256) grayscale 8-bit.

1: Convert fundus images to grayscale.

2: images resizing to 256 \* 256 grayscale 8-bit

3: Denoising image using mean filter

4: Images enhancement by applying CLAHE technology using equation (1).

$$pix = (p_{max} - p_{min}) * pix(f) + p_{min} \quad (1)$$

Where  $P_{max}$  and  $p_{min}$  stand for the maximum and minimum pixel values, respectively, while  $pix$  refer to the pixel value after CLAHE has been applied. Value of a picture, respectively, and  $Pix(f)$  reflects the cumulative probability distribution function after the clip limit has been reached. [26]

**Step 5:** Images normalization, each pixel is rescaled from the range [0-255] is changed to [0-1] by dividing each pixel by 255. This rescales each pixel so that it falls inside the range [0-1].

- 1. Image Resize:** A unified size is applied for all images supplied because of the size of images captured by a camera and submitted to various algorithms. The size of each image has been reduced so that it is exactly 256 by 256 pixels.
- 2. Grayscale Conversion:** All colored images are converted to grayscale. Colour image with three channels (RGB) slows processing operations. Each channel has the project's requirements. To speed up the process while keeping quality, all images are converted to grayscale.
- 3. Noise Reduction:** Image gathering and transmission introduce noise. Image enhancement is crucial to image processing. Mean filters average for all pixel mask performance to make unique pixel based on other pixels' intensities. This eliminates grain noises in processed image.
- 4. Images Enhancement:** Image enhancement aims to improve a source image by highlighting its differences. Image noise removal completes the repair process. CLAHE was utilized to pre-treat the fundus image to boost image contrast, as seen in figure 2.
- 5. Image Normalization:** An essential part of any pre-processing of images. Given that the CNN operates on images in the range [0-1], this is accomplished by rescaling each pixel from the range [0-255] into the range [0-1] using the division operator.

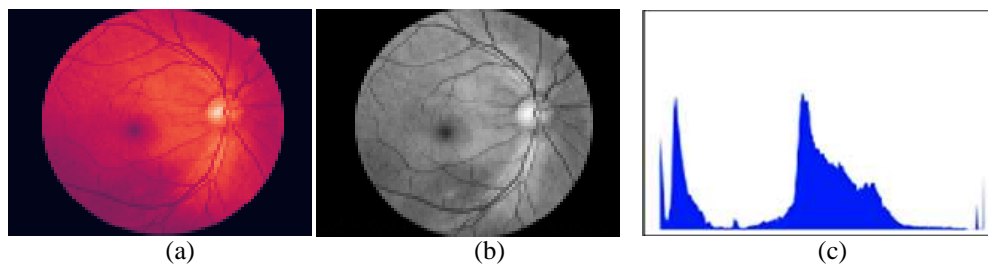


**Figure (2)** preprocessing process (a) Input image (b) CLAHE enhancement (c) Histogram after enhancement.

## B. Feature Extraction

It gives important information about a shape in a pattern, where a formal approach allows for easy access to the model's classification. With regards to processing images and pattern recognition. Extraction of features is a method of reducing the number of dimensions. Extracting primary features is done so as to learn the most important properties. This data will then be represented in lower dimensional areas. Attributes were extracted from the dataset's fundus images of glaucoma by employing CNN. A CNN's architecture includes numerous layers to optimize feature extraction. Table 4 presents the proposed structure of the CNN along with the input and output sizes.

## C. Classification

Features are extracted from retina images in a database to determine what information is most important to convey and to reduce the number of dimensions used to represent the data while making a glaucoma diagnosis. These collected features are used to create a classification that distinguishes glaucoma from healthy individuals. Through flatten layer is applied, a complete connection is made between a series of thinner structural layers, each of which contains an activation function (ReLU). The final layer is the dense layer, which is used for classification. Using a down-sampling procedure, the pooling layer decreases the size of the produced features, hence lowering the network's total processing cost [27]. Softmax is the most frequent last-layer activation function in CNNs. [28]. Following the Flatten layer, a fully connected dense layer with a ReLU activation function is employed. A dropout layer with a 0.2 ratio is included to regulate the network and prevent overfitting. The final diagnosis of glaucoma is determined in the output layer (Dense layer 2), which is fully connected. The output from this layer is processed by the SoftMax activation function to calculate probabilities for each category based on the input image. These probabilities are then used in the loss function to determine the error, which adjusts the network's weights via backpropagation during training. The CNN training employs the Adam optimization algorithm and the sparse

categorical cross-entropy loss function for evaluation. Learning rate reduction is applied when model performance plateaus, and early stopping is used to find the optimal number of epochs. Training involves preprocessing augmented data, with forward and backward passes across several epochs guided by early stopping to minimize error and adjust weights. The result is a set of trained weights and kernels for each layer, which are saved for use during testing. During testing, the CNN is evaluated using unseen test data, starting with preprocessing as outlined in Algorithm 1. The DCNN proposed structure contains the layers below:

1. **Convolutional 2D:** The first one start with conv. one. The layer will learn from 16 filters with size 3 by 3, no padding, and adapt “rectified linear activation function or ReLU” as the activation function. Where image with 256 by 256 are what this layer's gets as input. After each layer of convolution.
  2. **Maxpooling 2D:** The layer has a size of 2 by 2 and a stride equal 2. This is the max pooling layer. It's important to remember that you don't have to configure the input shape because it automatically done by the net based on the layer before it. In Max pooling, the Max value for the group of neurons in the layer below is used. The Max-pooling attribute was used to reduce the number of feature maps that came from earlier layers.
  3. **Convolutional 2D:** is also a convolutional layer. There are 32 filters with kernel of 3 by3, no-padding and the applied activation function is “ReLU”.
  4. **Maxpooling 2D:** The dimension of 2 by2, and stride with value of 2 utilized.
  5. **The Dropout:** A dropout regulation with a 0.2 rate used.
  6. **Convolutional 2D:** The convolutional kernel size 3 by 3, with no padding, and adapting “ReLU” as activating function.
  7. **Maxpooling 2D:** The max-pooling layer the stride is 2 and the size of a kernel is 2 by 2.
  8. **The Dropout:** Dropout regulation layer with a ratio of 0.20, and feed into the “fully connected layer”. The 3D feature maps converted into vectors.
  9. **The Flatten:** The output from the Max-pooling layer in the fifth block is a 2D matrix, which passes through a dropout layer and is reshaped via column scanning to form a one-dimensional vector. This vector is then fed into a fully connected layer.
  10. **Dense1:** The size of the output layer will be 128, and select motivated ReLU as activation.
  11. **Dense2:** Two units will be used in this layer (Nonglaucoma and glaucoma), and the Softmax was utilized.
- Table (3) shows the CNN Model details.

**Table (3)** CNN Model Details (sequential model)

Layer (type)	Output Shape	Param #
Conv 2D	(256,256,16)	160
Max-Pool-2D	(128,128,16)	0
Conv 2D	(128,128,32)	4640
Max-Pooling-2D	(64, 64, 32)	0
Dropout	(64, 64, 32)	0
Conv 2D	(64, 64, 64)	18496
Max-Pool-2D	(32, 32, 64)	0
Dropout	(32, 32, 64)	0
Flatten	(65536)	0
Dense1	(128)	8388736
Dense2	(2)	258
Total params	<b>8,412,290</b>	
Trainable params	<b>8,412,290</b>	

The next step is to process the images through the CNN architecture in a forward direction to extract features. This process utilizes the trained weights from the fully connected layers and the trained kernels from the convolutional layers, which were saved during training, the images are then classified as either glaucoma or normal in the test phase.

#### D. Evaluation Metrics

To assess the proposed method, various performance metrics were used, including Accuracy, Sensitivity, Specificity, and AUC. Multiple criteria were employed to evaluate the model's efficiency [29] [30]:

$$1. \text{ Accuracy (Acc): } = \frac{TPos + TNeg}{TPos + FPos + TNeg + FNeg} \quad (2)$$

$$2. \text{ Sensitivity (Sen): } Sen = \frac{TPos}{TPos + FNeg} \quad (3) \quad \text{Specificity (Spe): } Spe = \frac{TNeg}{TNeg + FPos} \quad (4)$$

Where  $TPos$ : TruePositive,  $FPos$ : FalsePositive,  $TNeg$ : TrueNegative,  $FNeg$ : FalseNegative.

3. Area Under Curve (AUC): The higher the AUC, the better the performance of the model at distinguishing between the positive and negative classes

$$AUC = \frac{\text{Sensitivity} + \text{Specificity}}{2} \quad (5)$$

#### 5. Results and Discussion

To prove the efficiency of a proposed system in terms of glaucoma diagnostic, we compare CNN predictions to a state-of-the-art reconstruction-based method. By applying the same setting for several datasets. A True positive is a diagnosis that is both correct (healthy) and classified as non-glaucoma (normal eye). Based on the sampled and analyzed photos from the ODIR datasets, a false positive diagnosis can be made (glaucoma classified as non-glaucoma (normal)). Negative diagnoses (such as an eye tested positive for glaucoma being classified as "normal") should be labelled "True negative," whereas "False negative" labels would be inaccurate (Normal categorized as glaucoma). The suggested system's classification report using ODIR datasets is displayed in Table (4).

**Table 4:** details of classification report for ODIR dataset

	<b>F1-score</b>	<b>Support</b>	<b>Precision</b>	<b>Recall</b>
Normal	0.980	165	0.970	0.990
Glaucoma	0.980	155	0.990	0.960
Accuracy	0.990	320		
Weighted Avg	0.980	320	0.980	0.980
Macro Avg	0.980	320	0.980	0.980

The proposed work was evaluated using the ODIR dataset, with 70% of the database coming was used to train the system, and 30% of the database was used to test the system performance. Macro-Avg is the mean average of precision/recall/F1 of all classes, while weighed-Avg is the total number of true positives of all classes divided by the total number of objects in all classes. In the conclusion, an impartial evaluation of the plan was carried out by making use of the test results. The (confusion matrix) that was used for the DCNN classification for the ODIR dataset is shown in Figure 3. The best accuracy of the proposed system, which is represented by the confusion matrix is accuracy: 0.9906; sensitivity: 1.00; specificity: 0.9806; and AUC: 0.9903.

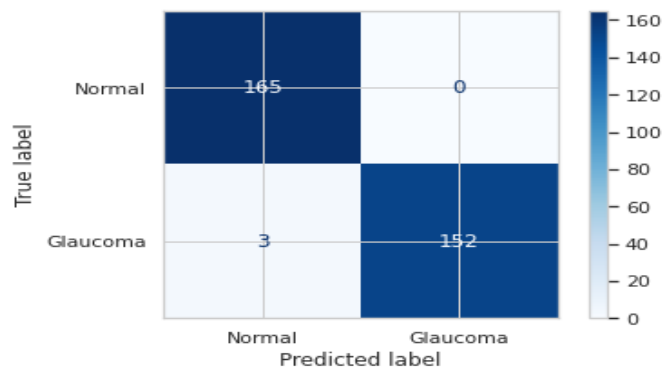


**Figure 3.** ODIR dataset's Confusion Matrix.

The ODIR dataset has 710 samples of fundus image in the train set and 320 samples in the test set; the obtained results in the training phase, loss: 0.0060 and accuracy: 1.00, and in the testing phase, loss: 0.0421 and accuracy: 0.9906. The accuracy and loss using the ODIR dataset is shown in Figures 4 below:

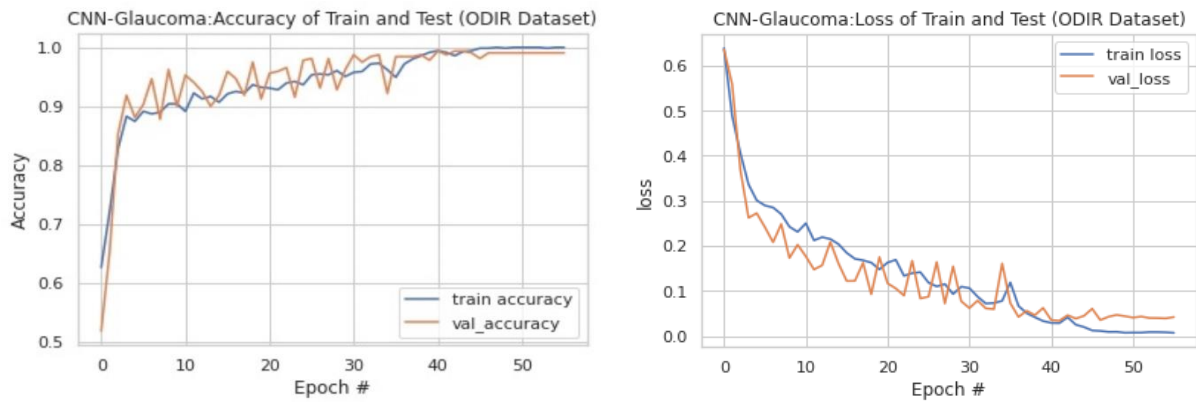


Figure 4. Accuracy and Loss for the ODIR dataset.

5.1 Results of SCES dataset

In the proposed system applied to the SCES data set, the training loss is 0.0239, and the training accuracy is 0.9941, while the test loss is 0.0126 and the test accuracy is 0.9960. The computed sensitivity is 1.0000, specificity: is 0.9048, and AUC is 0.9524. Figure (5) shows the confusion matrix, and Figures (6) shows the accuracy and loss obtained for the SCES dataset.

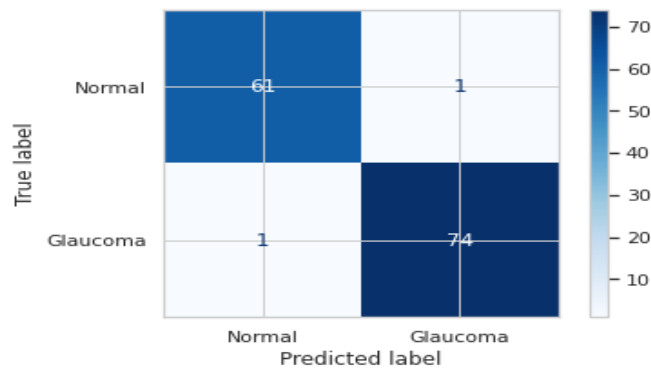


Figure (5) Confusion Matrix of SCES dataset

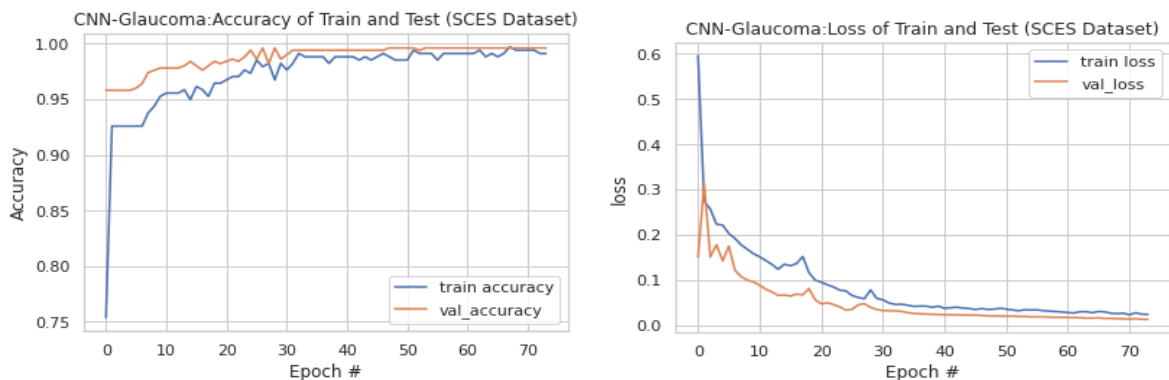


Figure 6. Accuracy and Loss for the SCES dataset.

### 5.2 Results for Rim One Dataset

The proposed system was applied on Rim one data set, which contained a total of 455 sample images and split into a training set 318 and a test set 137 (75 glaucoma, 62 average). The training loss is 0.0970, and the training accuracy is 0.9634, while the test loss is 0.0984, and the test accuracy is 0.9625. The computed sensitivity is 0.9839, specificity: is 0.9867, and AUC is 0.9853. Figure 7 show the confusion matrix and Figures 8 show the accuracy and loss obtained for Rim one dataset.

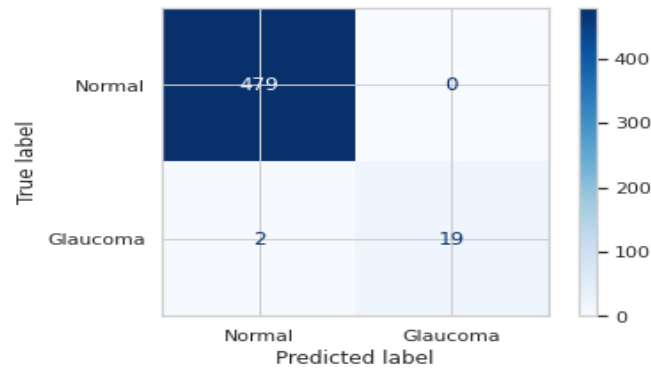


Figure 7. Confusion Matrix of Rim One dataset

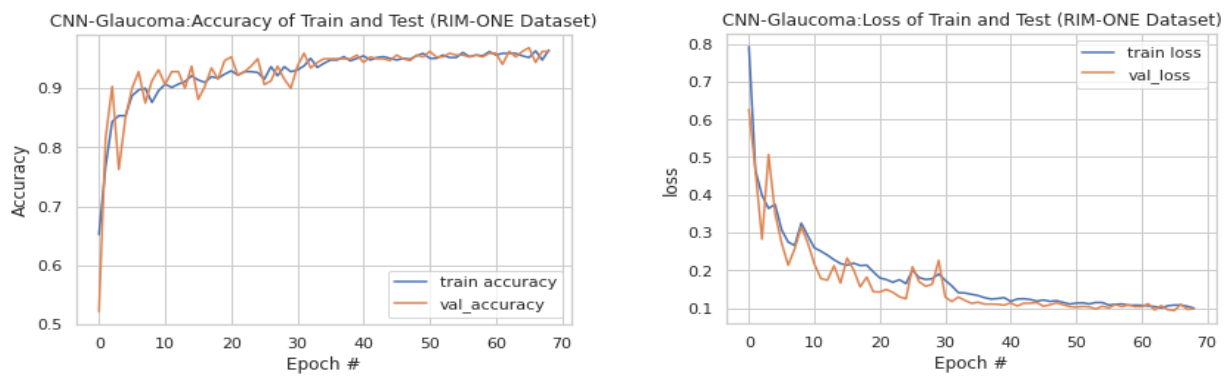


Figure 8. Accuracy and Loss for the RIM-ONE dataset.

### 5.3 Results for ACRIMA Dataset

The proposed system was applied to the ACRIMA data set, which contains a total of 705 sample images and split into a training set of 494 and a test set of 211 (110 glaucoma, 101 normal). The training loss is 0.0271 and the training accuracy is 0.9958, while the test loss is 0.0360 and the test accuracy is 0.9906. The computed sensitivity is 0.9839, specificity: is 0.9867, and AUC is 0.9853. Figure 9 show the confusion matrix of ACRIMA dataset and Figures 10 shows the accuracy and loss obtained for ACRIMA dataset.

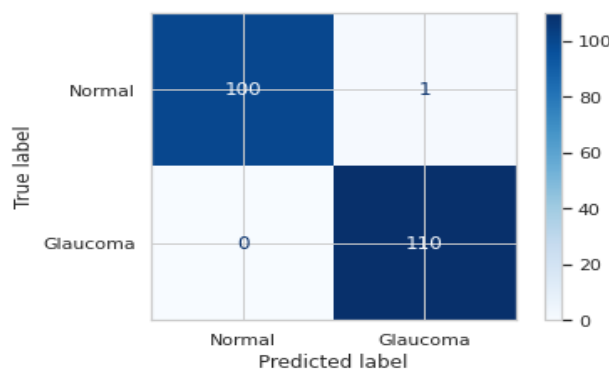


Figure (9) Confusion Matrix of ACRIMA dataset

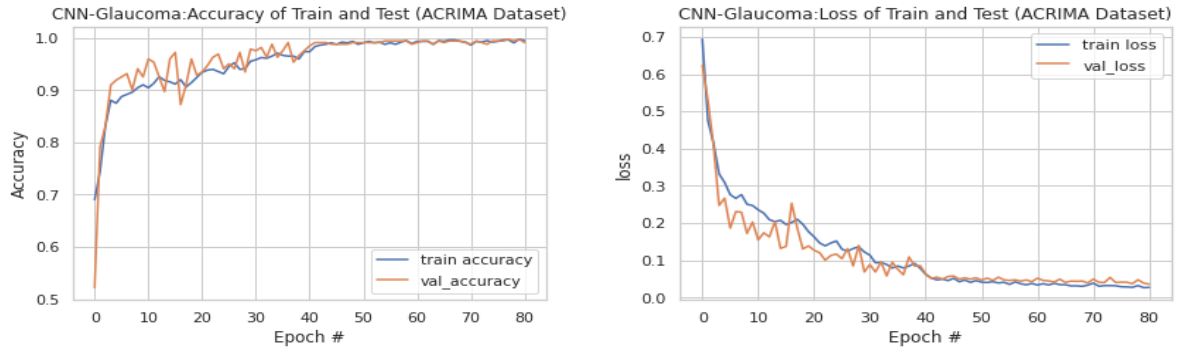


Figure 10. Accuracy and Loss for the ACRIMA dataset.

5.4 Results for Drishti-GS1 Dataset

The proposed system was applied to the Drishti-GS1 data set, which contains a total of 101 sample images and split into training set 71 and test set 30 (20 glaucoma, 10 normal). The training loss is 0.0408, and the training accuracy is 0.9915, while the test loss is 0.0877 and the test accuracy is 0.9719. The computed sensitivity is 1.0000, specificity: is 0.9500, and AUC is 0.9750. Figure 11 shows the confusion matrix for Drishti-GS1 dataset, and Figures 12 shows the accuracy and loss obtained for Drishti-GS1 dataset.

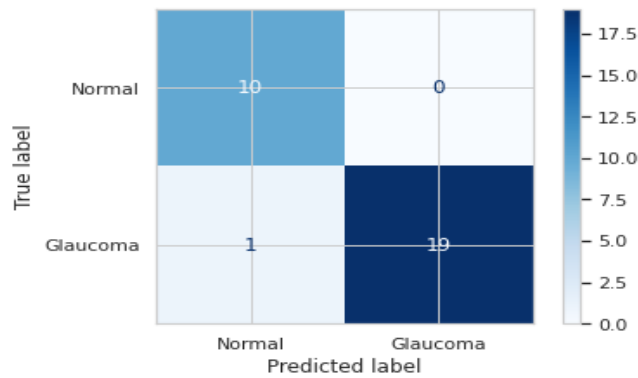


Figure 11. Confusion Matrix of Drishti-GS1 dataset

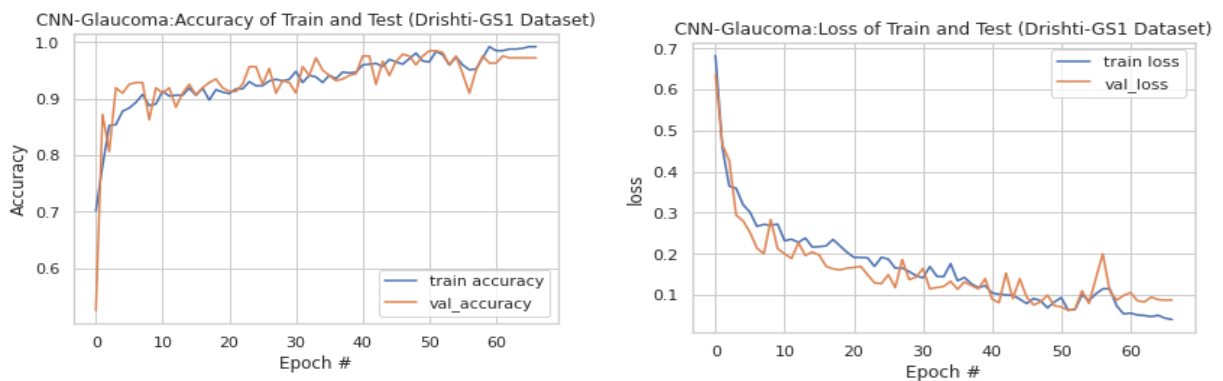


Figure 12. Accuracy and Loss for the Drishti-GS1 dataset.

5.5 Results for ORIGA dataset

The proposed system was applied to the ORIGA data set, which contains a total of 650 sample images, and split into a training set of 455 and a test set of 195 (85 glaucoma, 110 normal). The training loss is 0.0610, and the training accuracy is 0.9803, while the test loss is 0.0872 and the test accuracy is 0.9688. The computed sensitivity

is 0.9818, specificity: is 0.9882, and AUC is 0.9850. Figure 13 shows the confusion matrix for the ORIGA dataset, and Figures 14 shows the accuracy and loss obtained for the ORIGA dataset.

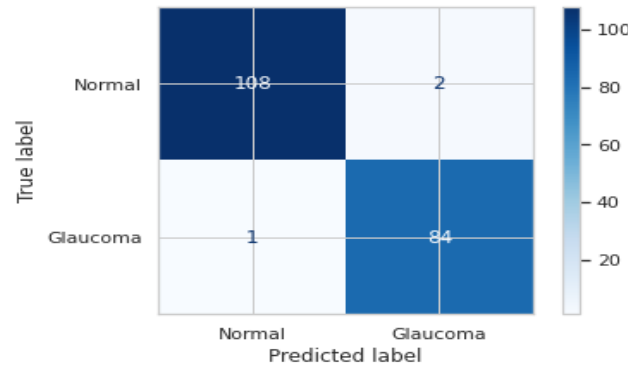


Figure 13. Confusion Matrix of ORIGA dataset

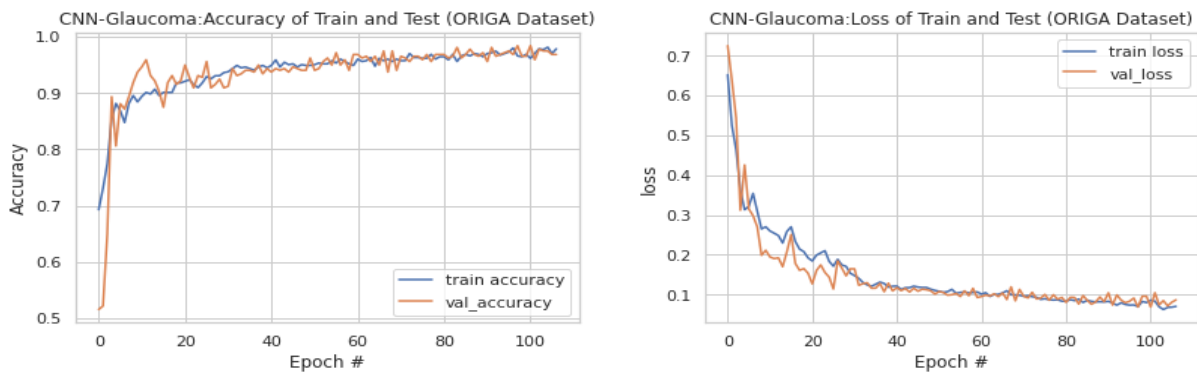


Figure (14) Accuracy and Loss for the ORIGA dataset.

The proposed system is applied to several datasets mainly ODIR dataset, then using ORIGA, DRISHTI-GS1, Rim one, HRF, and SCES, and the performance parameters are evaluated, such as Sensitivity, Accuracy, Area under the curve, and specificity. A higher accuracy ratio was obtained when using the SCES dataset about 0.996, as shown in figure 15. The proposed system is evaluated through make a comparison with a number of different deep learning algorithms for the diagnosis of glaucoma, and some of these algorithms make use of the same data set. It was discovered, through analysis of how the proposed method compares to earlier efforts, that the shows better performance accuracy. The average of the calculated results of Accuracy, Sensitivity, specificity, and AUC were computed for each dataset, and the obtained results were compared with the other methods, as the following Table (5).

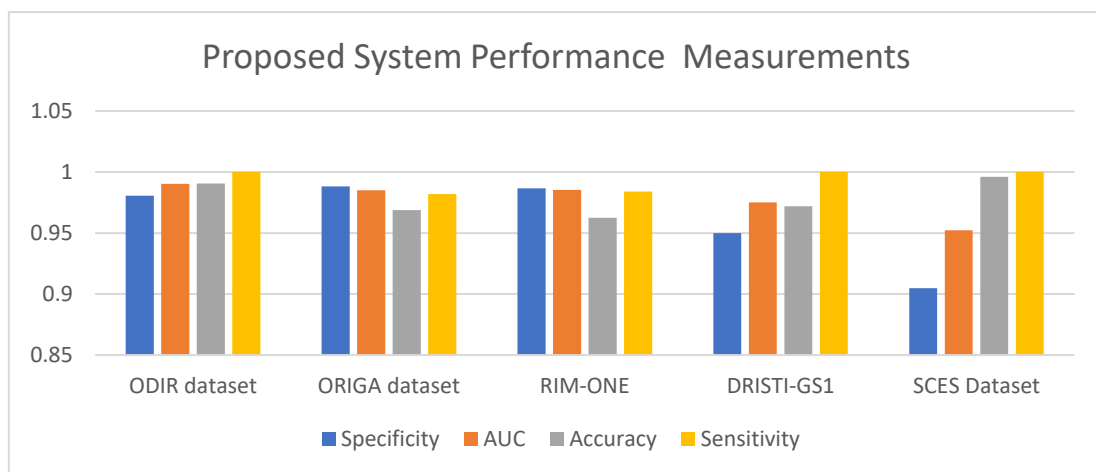


Figure 15. Proposed system performance measurement

**Table 5:** proposed model Comparison with various glaucoma detection methods

Author	Dataset	Specificity	AUC	Accuracy	Sensitivity
<b>Proposed CNN system</b>	ODIR dataset	0.9806	0.9903	0.9906	1
	ORIGA dataset	0.9882	0.985	0.9688	0.9818
	RIM-ONE	0.9867	0.9853	0.9625	0.9839
	DRISTI-GS1	0.95	0.975	0.9719	1
	SCES Dataset	0.9048	0.9524	0.996	1
<b>Ajitha S, M.V Judy et al, [10]</b>	HRF, Origa and DrishtiGS1			91.2100	
<b>Baidaa Al-Bander et al. [11]</b>	RIM-ONE	0.9080		0.8820	0.8500
<b>Gupta, R. K. et al. [12]</b>	SCES Dataset		0.8870		
	ORIGA Dataset		0.8310		
<b>Mary, J., [13]</b>	ORIGA Dataset		0.8310		
	SCES databases		0.8870		
<b>Ovrei, S., et al. [14]</b>	ImageNet			96.9500	
<b>Bajwa, M. Naseer, et al. [29]</b>	ORIGA dataset		86.8000		0.7100
<b>Chen, X. and et al. [31]</b>	ORIGA datasets		0.8310		
	SCES datasets		0.8870		
<b>Fu, Huazhu, et al.: MNet [32]</b>	SCES datasets	0.8706	0.8998	0.8157	0.7609
<b>Fu, Huazhu, et al. :DENet system [32]</b>	SCES datasets	0.8380	0.9183	0.8429	0.8478
<b>Oh, Sejong et al. [33]</b>	Gyeong sang National University Hospital	0.9500		0.9470	0.9410
<b>Soltani, A. et al. [34]</b>	Local Dataset 104 images			0.9615	
<b>Sreng, Syna, et al. [35]</b>	DRISTI-GS1		0.9206	0.9000	
	ORIGA dataset		0.8526	0.8000	
	REFUGE dataset		94.3200	0.9575	
	RIM-ONE dataset		99.0400	92.1100	
<b>Ramaida, Fira Mutia, et al. [36]</b>	Local Dataset			0.9400	
<b>Sang Phan et al. [37]</b>	KOSEI hospital dataset		0.9000		

## 6. Conclusion

This study puts out the idea of an automated glaucoma detection system that is powered by deep convolutional neural networks. In the beginning, a glaucoma data collection consisting of fundus images was pre-processed and improved so that the data set would be better suited for feeding the deep network. The preprocessing operation

increase the prediction accuracy. The suggested network investigated a variety of network layers, activation functions, loss functions, and optimization techniques in order to lessen the amount of processing required while keeping the same level of model accuracy. The SCES dataset yielded a classification accuracy of 0.996 percent, which was the best possible result. When evaluated beside other works of a same nature, this system did exceptionally well. Ophthalmologists were able to identify glaucoma more quickly and precisely with less network parameters thanks to this method, which was both very cost-effective and accurate. Additionally, there were fewer parameters, thus the method required less time.

## References

- [1] M. Chethan, C. Dasari, G. V. Uttarkar, and D. N. Sachin, "Diagnosis of Glaucoma using Machine Learning-A Survey," in 2019 Third International Conference on Inventive Systems and Control (ICISC), 2019, pp. 210-214. doi: 10.1109/ICISC44355.2019.9036462
- [2] S. Joshi, B. Partibane, W. A. Hatamleh, H. Tarazi, C. S. Yadav, and D. Krah, "Glaucoma Detection Using Image Processing and Supervised Learning for Classification," *Journal of Healthcare Engineering\**, vol. 2022, 2022. doi: 10.1155/2022/2988262.
- [3] "National Eye Institute," available: <https://nei.nih.gov/>. Accessed: Jun. 10, 2022.
- [4] S. Yu, D. Xiao, S. Frost, and Y. Kanagasigam, "Robust optic disc and cup segmentation with deep learning for glaucoma detection," *Computerized Medical Imaging and Graphics\**, vol. 74, pp. 61-71, 2019. doi: 10.1016/j.comp-medimag. 2019.02.005.
- [5] S. Palakvansa-Na-Ayudhya, T. Saphamrong, K. Sunthornwutthikrai, and D. Sakiyalak, "GlaucoVIZ: assisting system for early glaucoma detection using mask R-CNN," in *2020 17th International Conference on Electrical Engineering/Electronics, Computer, Telecommunications and Information Technology (ECTI-CON) \**, 2020, pp. 364-367. doi:10.1109/ECTI-CON49241. 2020. 9158128.
- [6] S. Y. Mohammed and M. Aljanabi, "From Text to Threat Detection: The Power of NLP in Cybersecurity," *Shifra: The Arabian Journal of Medicine and Surgery*, vol. 2024, pp. 1-8, Jan. 2024.
- [7] D. Shamia, S. Prince, and D. Bini, "An Online Platform for Early Eye Disease Detection using Deep Convolutional Neural Networks," in *2022 6th International Conference on Devices, Circuits and Systems (ICDCS)\**, 2022, pp. 388-392. doi: 10.1109/ICDCS54290.2022.9780765.
- [8] P. Jibhakate, S. Gole, P. Yeskar, N. Rangwani, A. Vyas, and K. Dhote, "Early Glaucoma Detection Using Machine Learning Algorithms of VGG-16 and Resnet-50," in *2022 IEEE Region 10 Symposium (TENSYP)\**, 2022, pp. 1-5. doi:10.1109/TENSYP54529.2022.9-864471.
- [9] V. S. Mary, E. B. Rajsingh, and G. R. Naik, "Retinal fundus image analysis for diagnosis of glaucoma: a comprehensive survey," *IEEE Access\**, 2016. doi: 10.1109/ACCESS.2016.2596761.
- [10] S. Ajitha, J. D. Akkara, and M. V. Judy, "Identification of glaucoma from fundus images using deep learning techniques," *Indian Journal of Ophthalmology\**, vol. 69, no. 10, pp. 2702, 2021. doi: 10.4103/ijo.IJO\_92\_21.
- [11] B. Al-Bander, W. Al-Nuaimy, M. A. Al-Tae, and Y. Zheng, "Automated glaucoma diagnosis using deep learning approach," in *2017 14th International Multi-Conference on Systems, Signals & Devices (SSD)\**, 2017, pp. 207-210. doi: 10.1109/SSD.2017.8166974.
- [12] R. K. Gupta, U. Sharma, and V. Singh, "Detection of Glaucoma using Deep Learning," *International Journal of Research in Engineering, Science and Management\**, vol. 5, no. 5, pp. 147-150, 2022. Available: <https://www.journals.resaim.com/ijresm/article/view/2072>.
- [13] A. S. Abdulbaqi, Q. H. Alsultan, S. M. Nejr, et al., "Design and Fabrication of Bio-Inspired Robotic Systems for Developed Mobility and Functionality in Unstructured Environments," *KHWARIZMIA*, vol. 2023, pp. 1-20, May 2023.
- [14] S. Ovreiu, I. Cristescu, F. Balta, A. Sultana, and E. Ovreiu, "Early detection of glaucoma using residual networks," in *2020 13th International Conference on Communications (COMM)\**, 2020, pp. 161-164. doi: 10.1109/COMM48946.2020.9141990.
- [15] J. I. Orlando, E. Prokofyeva, M. del Fresno, and M. B. Blaschko, "Convolutional neural network transfer for automated glaucoma identification," in *12th international symposium on medical information processing and analysis\**, vol. 10160, 2017, pp. 241-250. doi: 10.1117/12.2255740.
- [16] S. Serte and A. Serener, "A generalized deep learning model for glaucoma detection," in *2019 3rd International symposium on multidisciplinary studies and innovative technologies (ISMSIT)\**, 2019, pp. 1-5. doi: 10.1109/ISMSIT.2019.8932753.
- [17] M. T. Islam, S. A. Imran, A. Arefeen, M. Hasan, and C. Shahnaz, "Source and camera independent ophthalmic disease recognition from fundus image using neural network," in *2019 IEEE International Conference on Signal Processing, Information, Communication & Systems (SPICSCON)\**, 2019, pp. 59-63. doi: 10.1109/SPICSCON48833.2019.9065162.

- [18] L. K. Singh, H. Garg, M. Khanna, and R. S. Bhadoria, "An enhanced deep image model for glaucoma diagnosis using feature-based detection in retinal fundus," *Medical & Biological Engineering & Computing*, vol. 59, no. 2, pp. 333-353, 2021. doi: 10.1007/s11517-020-02307-5.
- [19] J. Wang, L. Yang, Z. Huo, W. He, and J. Luo, "Multi-label classification of fundus images with efficient net," *IEEE Access*, vol. 8, pp. 212499-212508, 2020. doi: 10.1109/ACCESS.2020.3040275.
- [20] Q. Abbas, "Glaucoma-deep: detection of glaucoma eye disease on retinal fundus images using deep learning," *International Journal of Advanced Computer Science and Applications*, vol. 8, no. 6, 2017. doi: 10.14569/IJACSA.2017.080606.
- [21] A. Budai, R. Bock, A. Maier, J. Hornegger, and G. Michelson, "Robust vessel segmentation in fundus images," *International journal of biomedical imaging*, vol. 2013, 2013. doi: 10.1155/2013/154860.
- [22] A. Diaz-Pinto, S. Morales, V. Naranjo, T. Köhler, J. M. Mossi, and A. Navea, "CNNs for automatic glaucoma assessment using fundus images: an extensive validation," *Biomedical Engineering Online*, vol. 18, no. 1, pp. 1-19, 2019. doi: 10.1186/s12938-019-0649-y.
- [23] F. Fumero, S. Alayón, J. L. Sanchez, J. Sigut, and M. Gonzalez-Hernandez, "RIM-ONE: An open retinal image database for optic nerve evaluation," in *2011 24th international symposium on computer-based medical systems (CBMS)*, 2011, pp. 1-6. doi: 10.1109/CBMS.2011.5999143.
- [24] H. J. Samawi, A. Y. Al-Sultan, and E. H. Al-Saadi, "Optic disc segmentation in retinal fundus images using morphological techniques and intensity thresholding," in *2020 International Conference on Computer Science and Software Engineering (CSASE)*, 2020, pp. 302-307. doi: 10.1109/CSASE48920.2020.9142061.
- [25] J. Sivaswamy, S. Krishnadas, S. Chakravarty, A. Uyyanonvara, A. Bagci, and J. M. R. Juarez, "A comprehensive retinal image dataset for the assessment of glaucoma from the optic nerve head analysis," *Journal of Medical Imaging*, vol. 3, no. 4, pp. 044002, 2016. doi: 10.1117/1.JMI.3.4.044002.
- [26] A. Shankaranarayana, M. Krishnadas, J. Sivaswamy, and A. Jain, "Fully convolutional networks for monocular optic disc and cup segmentation," *Biomedical Optics Express*, vol. 8, no. 8, pp. 4003-4017, 2017. doi: 10.1364/BOE.8.004003.
- [27] S. Mookiah, U. R. Acharya, R. J. Martis, A. Chandran, C. K. Chua, and E. Y. K. Ng, "A review of machine learning methods for retinal blood vessel segmentation and artery/vein classification," *Computer methods and programs in biomedicine*, vol. 145, pp. 67-107, 2017. doi: 10.1016/j.cmpb.2016.10.007.
- [28] J. L. Rodriguez, J. S. de Moura, D. Menotti, E. R. Barrero, and H. L. Silva, "Novel data augmentation technique for convolutional neural network in glaucoma diagnosis," *Journal of Imaging*, vol. 7, no. 2, pp. 33, 2021. doi: 10.3390/jimaging7020033.
- [29] A. A. Aldosari, R. Munir, and R. A. Elsheikh, "A Novel Glaucoma Detection Technique Using Deep Convolutional Neural Networks," *Applied Sciences*, vol. 10, no. 1, pp. 2020, 2020. doi: 10.3390/app10010256.
- [30] Z. Li, J. He, W. Chen, X. Zhao, and Z. Yang, "Automatic glaucoma diagnosis using deep learning algorithm based on disc and cup segmentation," in *2019 41st Annual International Conference of the IEEE Engineering in Medicine and Biology Society (EMBC)*, 2019, pp. 2002-2005. doi: 10.1109/EMBC.2019.8856708.